High-Precision Harmonic Analysis Algorithm Based on Five-Term MSD Second-Order Self-convolution Window Four-Spectrum Line Interpolation

Yang Qingjiang(✉) and Qu Xiangxiang

School of Electronics and Information Engineering, Heilongjiang University of Science and Technology, Harbin 150022, China
1962578365@qq.com

Abstract. For the frequency spectrum leakage and fence effect generated in Fast Fourier Transform (FFT) during asynchronous sampling and integral period truncation affect the precision of harmonic detection, a new algorithm for harmonic analysis based on four-spectrum-line interpolation FFT with second-order self-convolution window with five-term Maximum-Sidelobe-Decay (MSD) was proposed and the polynomial fitting method was used to construct the four-spectrum-line interpolation correction formula. The simulation results showed that this algorithm could improve the detection accuracy of amplitude, phase and frequency by 1-2 orders of magnitude compared with other commonly used windowed interpolation algorithms.

Keywords: Harmonic analysis · Five-term MSD self-convolution window · Four-spectrum line interpolation · Polynomial fitting

1 Introduction

With the development of industry, attention is turning to the harmonic problem caused by the widely used nonlinear load. In order to reduce harmonic pollution, accurate detection of harmonics becomes the primary issue [1]. The fast Fourier transform (FFT) algorithm has become a typical method of harmonic detection due to its characteristics of reliability, simplicity, fast operation speed, and easy implementation in hardware circuits [2]. However, when FFT is used for harmonic analysis, the asynchronous sampling and non-integral period truncation of the signal will cause spectrum leakage and fence effect, which will seriously affect the accuracy of harmonic detection [3]. In order to suppress the effects of spectral leakage and fence effects, a windowed interpolation correction algorithm can be used. At present, the commonly used window functions include Hanning window [4], Blackman window [5], Blackman-Harris window [6], Nuttall window [7], etc., all of which suppress the effect of spectrum leakage to a certain extent. The more commonly used interpolation algorithms are multimodal spectral line

X. Jiang and P. Li (Eds.): GreeNets 2020, LNICST 333, pp. 306–319, 2020.
https://doi.org/10.1007/978-3-030-62483-5_32

interpolation [8, 9], cubic spline interpolation [10–12], Lagrange interpolation [13–15], etc.

There are various FFT window interpolation algorithms nowadays [16], and the traditional single detection method cannot adapt to the increasingly complex harmonic detection requirements. At present, many researchers at home and abroad have conducted in-depth research on the harmonic detection algorithm where a new method is introduced on the basis of the original algorithm to realize the optimization of some calculation processes [17–19], or several methods are used to overcome the defects of a single detection algorithm [20–22]. Liu Kaipei and others have derived correction formulas for four typical window functions, verifying that the four-spectrum line interpolation algorithm has higher accuracy than the commonly used bispectral and trispectral lines [23]. Xie Qiang et al. Combined the five-term MSD window with the three-spectrum line interpolation algorithm, and compared with other commonly used window function interpolation algorithms, it has relatively higher accuracy [24]. Nan Xue et al. Proposed a four-spectrum line interpolation FFT harmonic analysis algorithm based on five MSD-Rife windows, and concluded that the five MSD-Rife windows with MSD/Rife weight ratio $\alpha/\beta = 0.6/0.4$ have better suppression of spectrum leakage Function [25]. In order to further improve the precision of windowed interpolation algorithm, the self-convolution of five-term MSD window was conducted in this paper to generate five-term MSD second-order self-convolution window. The information of bilateral symmetry lines of the peak frequency was taken into full consideration meanwhile in the harmonic analysis of four-spectrum-line interpolation FFT. Finally, a new algorithm for harmonic analysis was put forward based on four-spectrum-line interpolation FFT with second-order self-convolution window with five-term MSD.

2 Five-Term MSD Second-Order Self-convolution Window

2.1 Five-Term MSD Window Characteristics

In the case of asynchronous sampling, in order to reduce the influence of spectrum leakage on the harmonic measurement, a window function with a low sidelobe peak level and a high sidelobe attenuation rate is used for windowing the signal. The pentad MSD window is a cosine combination window [26], and its general form is

$$w(n) = \sum_{m=0}^{M-1} (-1)^m a_m \cos(\frac{2\pi mn}{N}) \tag{1}$$

In the formula: N is the number of sampling points; M is the number of terms of the window function; $m = 0, 1, 2, \ldots, M-1$; $n = 0, 1, 2, \ldots, N-1$; the coefficient of a_m should be meet constrains $\sum_{m=0}^{M-1} (-1)^m a_m = 0$ and $\sum_{m=0}^{M-1} (-1)^m a_m = 0$.

In the five-term maximum sidelobe attenuation window, the five coefficients of a_m are taken as $a_0 = 0.2734375$, $a_1 = 0.4375$,$a_2 = 0.221875$,$a_3 = 0.0625$, $a_4 = 0.0078125$, respectively.

According to its time domain information, the normalized logarithmic spectrum and the normalized logarithmic spectrum of several commonly used window functions are

drawn in the same graph, and the comparison graph is shown in Fig. 1. The specific sidelobe characteristics of the four window functions in Fig. 1 are shown in Table 1.

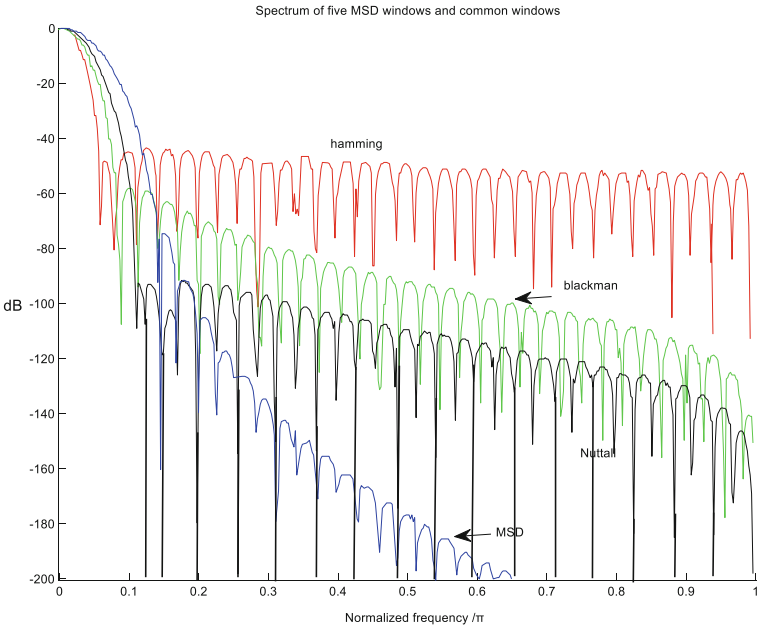

Fig. 1. The spectral characteristics of the window function.

Table 1. Sidelobe characteristics of each window function.

Window function name	Peak sidelobe/dB	Sidelobe decay rate/(dB/oct)
Hamming	−43	6
Blackman	−58	18
Nuttall	−83	24
Five-Term MSD	−75	54

With reference to Fig. 1 and Table 1, it can be seen that the five MSD window sidelobe peaks are −75 dB, and the sidelobe attenuation rate is 54 dB/oct. There is a clear advantage in the sidelobe attenuation rate, which is far greater than the other mentioned above. The window function has a very good attenuation effect on the side lobes, which can well suppress the influence of spectral leakage on other frequency points, and make the calculation result of the algorithm more accurate.

2.2 Five-Term MSD Self-Convolution Window

The self-convolution of the window function can improve the window function's ability to suppress sidelobe leakage and enhance the performance of the window function. In order to further improve the window function performance of the five-term maximum sidelobe attenuation window, the five-term MSD window is self-convolved And analyze the results of self-convolution.

Time-domain self-convolution of the five-term MSD windows yields

$$w_{MSD-p}(M) = \underbrace{w_{MSD}(N) * w_{MSD}(N) * \ldots * w_{MSD}(N)}_{p} \tag{2}$$

In the formula: p is the number of five MSD window functions participating in the self-convolution operation, which is also called the order of the self-convolution operation.

According to the convolution property, when two five-term MSD window sequences of length N are convolved, a sequence of length $2N-1$ can be obtained. Perform a zero-padding operation at the beginning or end of the sequence to obtain a sequence of $2N$ in length. Similarly, by performing $p-1$ convolution operations on five MSD window sequences of length N, a sequence of length $pN-p+1$ can be obtained. By adding $p-1$ zeros at the beginning or end, we can obtain Sequence of length pN.

From the discrete sequence Fourier transform, the frequency domain expression of the five-term MSD window is

$$W_{MSD}(\mathrm{w}) = \sum_{m=0}^{M-1} (-1)^m \frac{a_m}{2}\left[W_R(w - \frac{2m\pi}{N}) + W_R(w + \frac{2m\pi}{N})\right] \tag{3}$$

According to the nature of the convolution, the convolution in the time domain of the window function is equivalent to the product in the frequency domain, so the spectrum of the p-order five-term MSD self-convolution window is

$$W_{MSD-\mathrm{p}}(\mathrm{w}) = [W_{MSD}(w)]^p \tag{4}$$

The main lobe width of the p-order pentad MSD self-convolution window, that is $W_{MSD-\mathrm{p}}(w)$, the point at which 0 is taken for the first time, which $|W_{MSD}(\mathrm{w})|$ is 0 at this time.

According to formula (3),

$$\begin{cases} \frac{N}{2}\left(\mathrm{w} \pm \frac{2\pi \mathrm{m}}{N}\right) = d\pi \\ \\ \frac{1}{2}\left(w \pm \frac{2\pi m}{N}\right) \neq d\pi \end{cases} \quad d = 0, \pm 1, \pm 2 \cdot \cdot \tag{5}$$

Since the main lobe of the five MSD self convolution windows is $W_{MSD}(\mathrm{w})$ the point of the first 0, at this time, $d = \pm 1$, the main lobe width of the five MSD self convolution windows is

$$B_{MSD-p} = \frac{20\pi}{N} = \frac{20\pi p}{M} \tag{6}$$

From Eq. (6), the main lobe width of the p-order pentad MSD self-convolution window is inversely proportional to the length of the mother window. When the length M of the p-order pentad MSD self-convolution window is constant, the main lobe width of the p-order pentagonal MSD self-convolution window depends only on the convolution order p. The higher the convolution order, the larger the main lobe width, The lower the frequency resolution.

From Eq. (4), we construct first-order, second-order, and fourth-order pentad MSD self-convolution windows, and the corresponding spectrum curves are shown in Fig. 2.

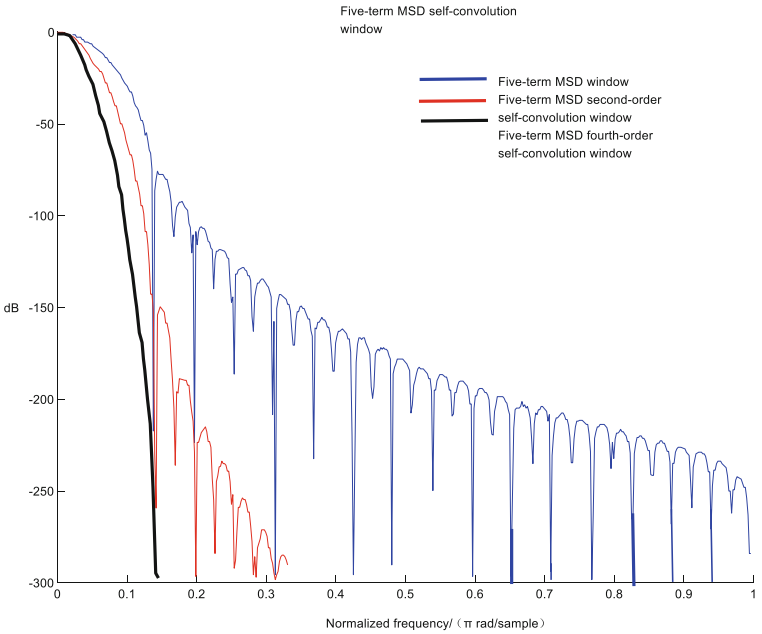

Fig. 2. Spectrum of five MSD self-convolution windows

It can be seen from Fig. 2 that with the increase of the self-convolution order of the five-term cosine self-convolution window, the sidelobe peak value gradually decreases, and the sidelobe attenuation gradually increases. The sidelobe peak of the second-order self-convolution window is −151.56 dB, the sidelobe peak of the fourth-order self-convolution window is −303.12 dB, and the sidelobe attenuation speed of the second-order self-convolution window is 108 dB/oct, and the fourth-order is 216 dB./oct. However, as the order p increases, the length of the convolution window will increase to p times the mother window. If the length of the sampling window is maintained, according to formula (6), the main lobe width will increase to the original p times. The main lobe width of the second-order self-convolution window is $40\pi/M$, but the fourth-order self-convolution window will reach $80\pi/M$. Although the rapid attenuation of the side-lobe peaks is conducive to the improvement of the calculation accuracy, too large the main

lobe width will have a great impact on the resolution. Large, so we choose the five-term MSD second-order self-convolution window as the window function in harmonic detection.

3 Four-Spectrum Interpolation Algorithm

Taking a single frequency signal as an example for analysis, let $x(t)$ take the discrete time signal sampled uniformly at the sampling frequency f_s as:

$$x(n) = A_0 \sin(2\pi \frac{f_0}{f_s} n + \phi_0) \tag{7}$$

Where: A_0 is the amplitude of the signal; f_0 is the frequency of the signal; ϕ_0 is the initial phase angle of the signal; f_s is the sampling frequency, $n = 0, 1, 2, \cdots, N-1$,

where N is the number of sampling points.

Windowing truncation of the signal $x(n)$ using the p-order pentad maximum sidelobe attenuation self-convolution window will obtain $x_w(n) = x(n) \times w(n)$,$x_w$ is calculated in the frequency domain as

$$X_w(e^{jw}) = \sum_{n=0}^{N-1} x(n)w(n)e^{-jwn}$$
$$= \frac{A_0}{2j}\left[e^{j\phi_0} W(\frac{2\pi(f-f_0)}{f_s}) - e^{-j\phi_0} W(\frac{2\pi(f+f_0)}{f_s})\right] \tag{8}$$

Ignoring the effect of the long-spectrum leakage at the frequency $-f_0$, the DFT transform of $x_w(n)$'s DTFT transform $X_w(k)$ of $X_w(e^{jw})$ is sampled at equal intervals $\Delta w = \frac{2\pi}{N}$:

$$X_w(k) = \frac{A_0}{2j} e^{j\phi_0} W(k - \frac{f_0}{\Delta f}) \tag{9}$$

Where $\Delta f = \frac{f_s}{N_c}$, $k = 0, 1, 2, \cdots, N-1$, $W(k)$ is the spectral function of the p-order pentad MSD self-convolution window. Because of the sampling point $N \rangle\rangle 1$, the expression of $W(k)$ is:

$$W(k) = \left\{\frac{N}{\pi} e^{-j\frac{k\pi}{p}} \sin(\frac{k\pi}{p})\left[\sum_{m=0}^{M-1} (-1)^m \frac{a_m k}{(k)^2 - p^2 m^2}\right]\right\}^p \tag{10}$$

In asynchronous sampling, the signal frequency $f = k\Delta f$ is difficult to be located at the sampling frequency point, that is, k is generally not an integer, and the FFT generates a spectrum leakage at this time. As shown in Fig. 3, the four spectral lines near the peak frequency k are k_1,k_2,k_3,k_4 and $k_1 < k_2 = k_1 + 1 < k_3 = k_2 + 1 < k_4 = k_3 + 1$, respectively. Let $\varepsilon = k - k_2 - 0.5$, because of $0 \le k - k_2 \le 1$,so $\varepsilon \in [-0.5, 0.5]$, find ε is a key step to accurately estimate the harmonic parameters.

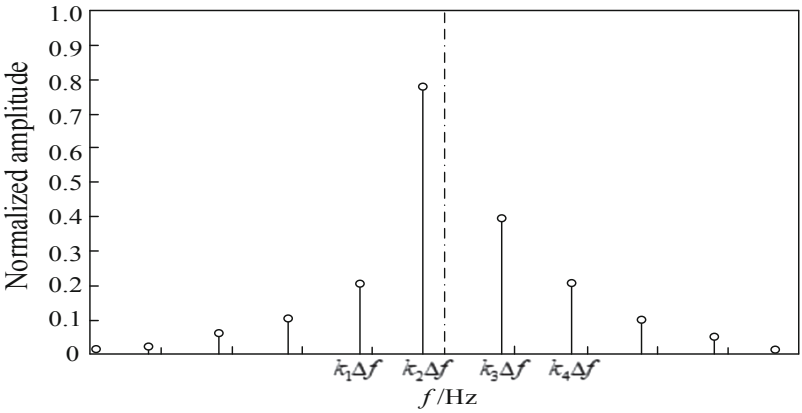

Fig. 3. FFT spectrum under asynchronous sampling

Record the amplitudes of the four spectral lines, respectively:$y_1 = |X_w(k_1)|$, $y_2 = |X_w(k_2)|$, $y_3 = |X_w(k_3)|$, $y_4 = |X_w(k_4)|$. Let $R = (2y_3 + y_4)$,$S = (2y_2 + y_1)$. Then according to formula (9) and bringing in ε, we get:

$$r = 2|W(-\varepsilon + 0.5)| + |W(-\varepsilon + 1.5)| \tag{11}$$

$$s = 2|W(-\varepsilon - 0.5)| + |W(-\varepsilon - 1.5)| \tag{12}$$

Let

$$\gamma = \frac{y_3 + y_4 - y_1 - y_2}{y_3 + y_4 + y_1 + y_2} \tag{13}$$

Then

$$\gamma = \frac{r - s}{r + s} \tag{14}$$

It can be seen from Eq. (14) that γ is a function of ε and $\gamma = g(\varepsilon)$, and the inverse function $\varepsilon = g^{-1}(\gamma)$ can be obtained to find the offset ε. Polynomial approximation can be used to calculate $\varepsilon = g^{-1}(\gamma)$. Use Matlab's polyfit function to fit the inverse function. If you fit $2q + 1$ times, you get:

$$\varepsilon \approx L(\gamma) = a_1\gamma + a_3\gamma^3 + \cdots + a_{2q+1}\gamma^{2q+1} \tag{15}$$

Where $a_1, a_3, \cdots, a_{2q+1}$ is an odd-order coefficient.

After finding ε, the frequency correction formula of the available signal is:

$$f = k\Delta f = (k_2 + 0.5 + \varepsilon)f_s/N \tag{16}$$

The phase correction formula of the signal is:

$$\phi_0 = \arg[X_w(k_2)] + \frac{\pi}{2} - \arg[W(-\varepsilon - 0.5)] \tag{17}$$

It can be seen from Fig. 3 that the position of k_2,k_3 is closer to k, so the two spectral lines are given greater weight, that is, the weights of k_1,k_2, k_3,k_4,and are added 1, 2, 2, and 1, respectively. The amplitude estimation formula is:

$$A_0 = \frac{2(y_1 + 2y_2 + 2y_3 + y_4)}{r + s} \tag{18}$$

When N is 512 or 1024, Eq. (18) can be simplified as $A_0 = N^{-p}(y_1 + 2y_2 + 2y_3 + y_4)u(\varepsilon)$,Where $u(\cdot)$ is an even function, so the approximation polynomial of the magnitude is:

$$A_0 = N^{-p}(y_1 + 2y_2 + 2y_3 + y_4) \cdot (a_0 + a_2\varepsilon^2 + \cdots + a_{2q}\varepsilon^{2q}) \tag{19}$$

In the formula, $a_0, a_2, \cdots, a_{2q}$ is an even term coefficient.

The frequency domain expression of the P-order pentad MSD self-convolution window can be simplified by formula (10), where M = 5.

$$|W(k)| = \left[\frac{N}{\pi}\left|\sin(\frac{k\pi}{p})\sum_{m=0}^{4}(-1)^m\frac{a_m k}{k^2 - p^2m^2}\right|\right]^p \tag{20}$$

Substituting Eq. (20) into Eq. (14), randomly taking a set of ε from $[-0.5, 0.5]$ and substituting it will get a corresponding set of γ values. The number of ε cannot be too small, otherwise it will affect the fitting accuracy.$\varepsilon \approx L(r)$ is obtained by a polynomial fitting function polyfit(γ, ε, i), where i represents the degree of fitting (i usually takes 5 or 7 times).

Take the fitting number $i = 7$, and the corresponding ε of the second-order pentad MSD self-convolution window is:

$$\varepsilon \approx L(\gamma) = 0.3000500\gamma^7 + 0.4966542\gamma^5 + 1.0904182\gamma^3 + 5.7181015\gamma \tag{21}$$

The Eq. (18) is combined with the Eq. (20), and the coefficient of $u(\varepsilon)$ is fitted by *polyfit*(ε, $u(\varepsilon)$, i).

$$\begin{aligned} u(\varepsilon) = {} & 0.002803784\varepsilon^6 + 0.084853287\varepsilon^4 \\ & + 1.794230810\varepsilon^2 + 19.639067884 \end{aligned} \tag{22}$$

4 Simulation Experiment Analysis

In order to verify the accuracy of the algorithm in this paper, a 21st harmonic simulation analysis is performed. The signal model of the simulation sampling is:

$$x(n) = \sum_{i=1}^{21} A_i \sin(2\pi in\frac{f_1}{f_s} + \theta_i) \tag{23}$$

The amplitudes A_i of each harmonic and the phase θ_i of each harmonic are shown in Table 2. The fundamental frequency f_1 of the signal is 50.5, the sampling frequency f_s is 2520, and the number of sampling points N is 512.

Table 2. Fundamental and harmonic parameters of harmonic signals

Harmonic order	1	2	3	4	5	6	7
Amplitude/V	220	4.4	10	3	6	2.1	3.2
Phase/(∘)	0.05	39	60.5	123	−52.7	146	97
Harmonic order	8	9	10	11	12	13	14
Amplitude/V	1.9	2.3	0.8	1.1	0.7	0.85	0.1
Phase/(∘)	56	43.1	−19	4.1	40	10.5	115
Harmonic order	15	16	17	18	19	20	21
Amplitude/V	1	0.06	0.4	0.04	0.3	0.005	0.01
Phase/(∘)	25	53.1	−132	85	0.8	53	−72

Window the signal model given by Eq. (23), and then perform simulation experiments according to the flow of Fig. 4.

Hanning window and Blackman-Harris (B-H) window four-line interpolation uses the correction formula given in Literature [23], five-term MSD window three-line interpolation uses the correction formula given in Literature[24], and five-term MSD window four-line interpolation uses literature The correction formula given in [25]. The five-term MSD second-order self-convolution window four-spectrum line interpolation uses the correction formula of this paper. Through comparison of simulation experiments, the relative errors of amplitude, phase and frequency are shown in Figs. 5, 6 and 7.

It can be seen from the simulation results that:①under the same conditions, compared with Hanning window and Blackman Harris window, the harmonic detection accuracy of the five MSD windows is higher, and the relative error of amplitude, phase and frequency is increased by about 3–4 orders of magnitude; ② compared to the five-term MSD window of the five-term MSD second-order self-convolution window, the relative errors in amplitude, phase, and frequency have increased by about 1–2 orders of magnitude; ③ on the premise of adding phase and window function, the accuracy of harmonic detection can be improved by four spectral line interpolation compared with three spectral line interpolation, which can be increased by 1–2 orders of magnitude.

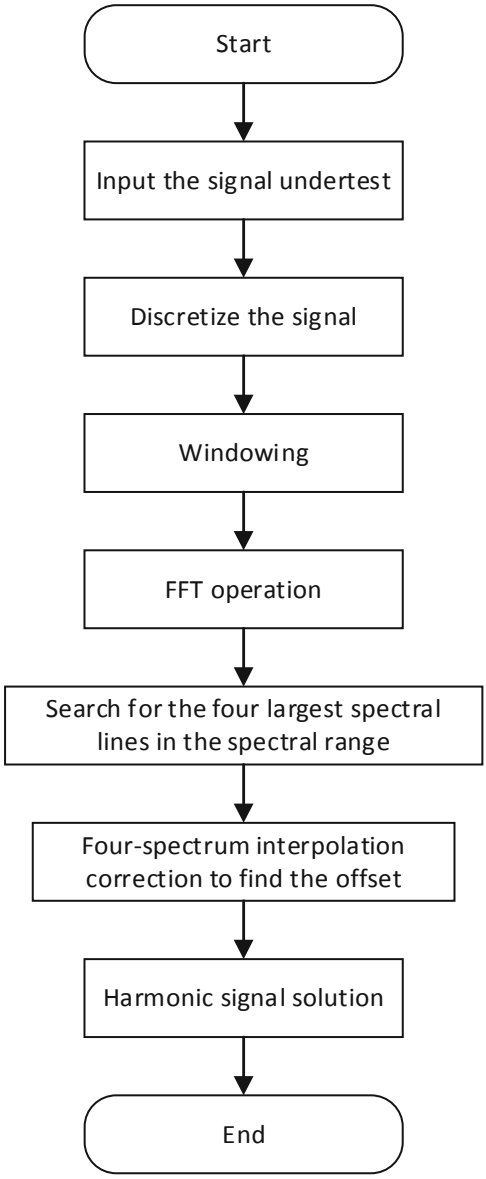

Fig. 4. Flow chart of simulation experiment program

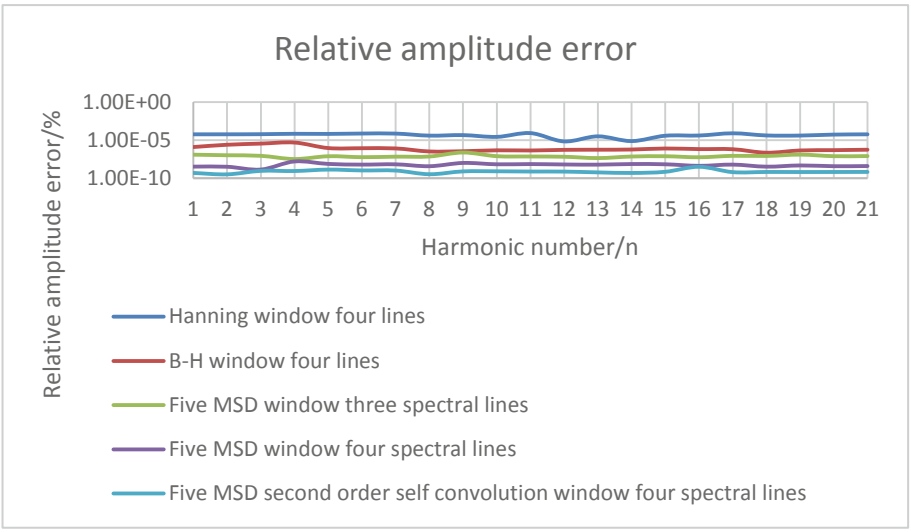

Fig. 5. Relative error of amplitude for different windowed interpolation algorithms

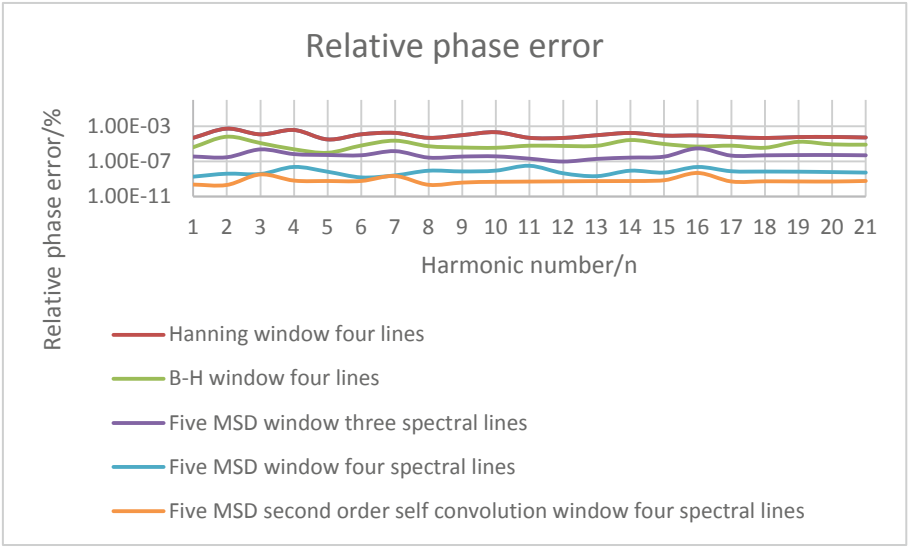

Fig. 6. Relative error of phase for different windowed interpolation algorithms

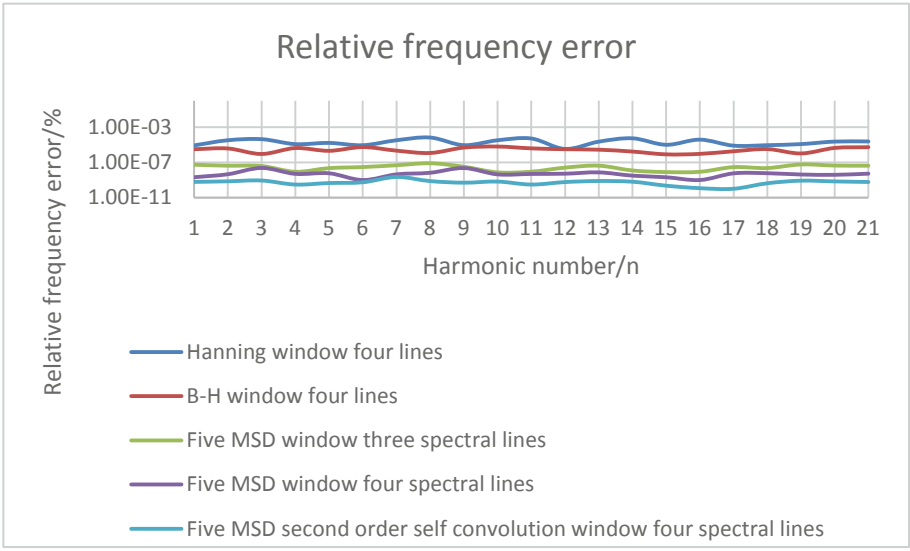

Fig. 7. Relative error of frequency for different windowed interpolation algorithms

5 Conclusion

In this paper, five-term MSD window with superior sidelobe performance were selected to construct five-term MSD self-convolution window. By analyzing their spectrum characteristics, it was concluded that the sidelobe performance of the five-term MSD self-convolution window was getting better with the increase of the convolution order, and the width of the main lobe also increased gradually. On this basis, a new algorithm for harmonic analysis based on four-spectrum-line interpolation FFT with second-order self-convolution window with five-term MSD was proposed, and the correction formulas of various parameters were calculated to realize the high-precision detection of amplitude, frequency and phase of each harmonic in the signal. Compared with other algorithms, this algorithm greatly improved the accuracy of harmonic detection and could be applied to the occasions where the accuracy of harmonic analysis were demanding.

References

1. Wen, H., Teng, Z.S., Guo, S.Y.: Triangular self-convolution window with desirable side lobe behaviors for harmonic analysis of power system. IEEE Trans. Instrum. Meas. **59**(3), 543–552 (2010)
2. Zeng, B.: Parameter estimation of power system signals based on cosine self-convolution window with desirable side-lobe behaviors. IEEE Trans. Power Delivery **26**(1), 250–257 (2011)
3. Nuttall, A.: Some windows with very good sidelobe behavior. IEEE Trans. Acoustics, Speech, Signal Process. **29**(1), 84–91 (2003)
4. Wen, H., et al.: Hanning self-convolution window and its application to harmonic analysis. Sci. China Ser. E: Technol. Sci. **52**(2), 467 (2009)

5. Kumar, A.: A comparative study of performance of blackman window family for designing cosine-modulated filter bank. In: (IACSIT—International Association of Computer Science and Information Technology) Proceedings of International Conference on Circuits, System and Simulation (ICCSS 2011) (IACSIT—International Association of Computer Science and Information Technology), pp. 315–321 (2011)
6. Agre, D.: Interpolation in the frequency domain to improve phase measurement. Measurement **41**(2), 151–159 (2008)
7. Zhu, Y., Wang, Y., Lin, T., Feng, C., Chen, J., Gao, Y.: Harmonic analysis of power system based on nuttall self-convolution window triple-spectral-line interpolation FFT. In: Proceedings of the 2017 2nd International Conference on Control, Automation and Artificial Intelligence (CAAI 2017) (2017)
8. Agrez, D.: Weighted multipoint interpolated DFT to improve amplitude estimation of multifrequency signal. IEEE Trans. Instrum. Meas. **51**(2), 287–292 (2002)
9. Song, X., Li, D., Li, Z., Guo, W.: Harmonic analysis and simulation study using triple-spectrum-line interpolation fft algorithm. In: Proceedings of the 2015 International Conference on Materials Engineering and Information Technology Applications (2015)
10. Bogdanov, V.V., Volkov, Y.S.: Shape-preservation conditions for cubic spline interpolation. Siberian Adv. Math. **29**(1), 231 (2019)
11. Idais, H., Yasin, M., Pasadas, M., González, P.: Optimal knots allocation in the cubic and bicubic spline interpolation problems. Math. Comput. Simul. **164**, 131 (2019)
12. Li, H., Li, L., Di Zhao, : An improved EMD method with modified envelope algorithm based on C2 piecewise rational cubic spline interpolation for EMI signal decomposition. Appl. Math. Comput. **335**, 112 (2018)
13. de Camargo, A.P.: On the numerical stability of Newton's formula for Lagrange interpolation. J. Comput. Appl. Math. **365**, 112369 (2019)
14. Kobayashi, K., Tsuchiya, T.: Error analysis of Lagrange interpolation on tetrahedrons. J. Approximation Theory **249**, 105302 (2020)
15. Keller, W., Borkowski, A.: Thin plate spline interpolation. J. Geodesy **93**(9), 1251 (2019)
16. Li, P., Wei, Z., Lei, C., Songling, H.: Research on the performance comparison of harmonic analysis algorithms for power grid signals. Electr. Meas. Instrum. **57**(01), 1–20 (2020)
17. Wen, H., Teng, Z., Wang, Y., et al.: Optimized trapezoid convolution windows for harmonic analysis. IEEE Trans. Instrum. Meas. **62**(9), 2609–2612 (2013)
18. Junmin, Z., Kaipei, L., Li, W., et al.: An algorithm for harmonic analysis based on multiplication window function. Power Syst. Prot. Control **44**(13), 1–5 (2016)
19. Wang Ling, X., Baiyu, S.C., et al.: An approach for harmonic analysis based on a new type of cosine combination window interpolation FFT. Wuhan Univ. J. **47**(2), 250–254 (2014)
20. Candan, Ç.: A method for fine resolution frequency estimation from three DFT samples. IEEE Signal Process. Lett. **18**(6), 351–354 (2011)
21. Duda, K.: DFT interpolation algorithm for Kaiser-Bessel and Dolph-Chebyshev windows. IEEE Trans. Instrum. Meas. **60**(3), 784–790 (2011)
22. Li, Y.F., Chen, K.F.: Eliminating the picket fence effect of the fast fourier transform. Comput. Phys. Commun. **178**(7), 486–491 (2008)
23. Junmin, Z., Kaipei, L., Li, W., Wenjuan, C.: A rapid algorithm for harmonic analysis based on four-spectrum-line interpolation FFT. Power Syst. Prot. Control **45**(01), 139–145 (2017)
24. Shi, L., Xie, Q., Ma, X.: High accuracy analysis of harmonic algorithm based on 5-term maximum-sidelobe-decay window and triple-spectrum-line interpolation. Power Syst. Prot. Control **45**(07), 108–113 (2017)

25. Xue, N., Shulian, Y., Tianze, L., Jiazhen, Q.: Electrical harmonic analysis based on five-term MSD-rife window and four-spectrum-line interpolation FFT. Hydropower Energy Sci. **36**(10), 177–180 (2018)
26. Song, S., Ma, H., Xu, G., Wang, F., Wang, J.: Power harmonic analysis based on 5-term maximum-sidelobe-decay window interpolation. Autom. Electr. Power Syst., **39**(22), 83–89 + 103 (2015)